

NILU  
TEKNISK NOTAT NR 7/77  
REFERANSE: 01474  
DATO: SEPTEMBER 1977

EFFECT OF DEPOSITION ON VERTICAL  
CONCENTRATION DISTRIBUTION FROM  
A GROUND LEVEL SOURCE\*

BY

Y. GOTAAS AND A.R. TINDERHOLT

\*Reprint of Teknisk Notat VM-112, Oct. 1973,  
with permission from the Norwegian Defence  
Research Establishment.

NORWEGIAN INSTITUTE FOR AIR RESEARCH  
P.B. 130 N-2001 LILLESTRØM  
NORWAY

CONTENTS

	Page
1 INTRODUCTION	3
2 SEMI-EMPIRICAL DIFFUSION EQUATION	3
3 NUMERICAL COMPUTATION SCHEME	5
3.1 Pseudodiffusion	7
4 EXAMPLE	8
References	11
Appendix - Computing Technique	12

EFFECT OF DEPOSITION ON VERTICAL CONCENTRATION DISTRIBUTION  
FROM A GROUND LEVEL SOURCE

1 INTRODUCTION

Turbulent diffusion of gases and particles released into the atmosphere has become of increasingly practical importance. Of special interest is the dispersion in the surface boundary layer.

We may estimate concentration distribution with help of semi-empirical diffusion equations. In the real atmosphere the height dependence of wind velocity and eddy diffusivities can then not be neglected. Analytical solutions do only exist when we express these parameters as power functions of the height, but not when we also consider deposition to the ground. We here present a numerical method, primarily with the object to study the effect of deposition. A ground source of finite duration is selected.

2 SEMI-EMPIRICAL DIFFUSION EQUATION

We assume a stationary flow with mean wind along the OX-axis of a cartesian coordinate system. The wind velocity,  $u$ , and eddy diffusivities are assumed only dependent on height, and the principal axes of the diffusivity tensor,  $K_{ij}$ , to coincide with the coordinate axes. The semi-empirical diffusion equation, without sources or sinks in the space considered, can then be written (1, p 613)

$$\frac{\partial C}{\partial t} + u(z) \frac{\partial C}{\partial x} = K_x \frac{\partial^2 C}{\partial x^2} + K_{yy} \frac{\partial^2 C}{\partial y^2} + \frac{\partial}{\partial z} (K_{zz} \frac{\partial C}{\partial z}) \quad (1)$$

where  $C$  = concentration in mass units per unit volume. The along wind eddy diffusion is usually much smaller than the advective term and is therefore neglected.

We are primarily interested in how the maximum ground level concentrations and vertical concentration distributions are effected by deposition. Height dependence of mean lateral concentration has the same shape as that of the maximum concentration in the  $OZ$ -plane at a fixed distance, and with symmetric horizontal distribution. Consequently, we may study this height dependence using the 2-dimensional diffusion equation, valid for a line source along the  $OY$ -axis. To simplify boundary conditions, we use a release of finite time,  $T$ . Our semi-empirical diffusion equation, with  $K_{zz} = K$ , reads

$$\frac{\partial C(x,z,t)}{\partial t} = -u(z) \frac{\partial C(x,z,t)}{\partial x} + \frac{\partial}{\partial z} \left[ K(z) \frac{\partial C(x,z,t)}{\partial z} \right] + q(x,z,t) \quad (2)$$

with the boundary conditions

$$C(x,y,t) \Big|_{t=0} = 0 \text{ for all } x \text{ and } z \neq 0$$

$$K \frac{\partial C}{\partial z} \Big|_{z=0} = R \cdot C(x,0,t)$$

$$q(0,0,t) = \text{const for } 0 \leq t \leq T, \text{ otherwise } q = 0$$

Deposition is assumed proportional to the ground level concentration,  $C(x,0)$ . The factor  $R$  has dimension of velocity and is named deposition velocity. (Fallout of particles by gravitational settling can be included by adding a term  $-w \frac{\partial C}{\partial z}$  to the left side of equation (2), where  $w$  then is the settling velocity.)

3 NUMERICAL COMPUTATION SCHEME

Equation (2) is a 2-dimensional parabolic equation with variable coefficients. A simple explicit difference formula is used to solve our initial value problem.

We adopt a grid that covers a part of the 2-dimensional space, with grid steps  $\Delta x$  and  $\Delta z$ . The mass concentration in a cell is  $C_{i,j}^t$ , where  $t$  denotes the current time and indexes  $i$  and  $j$  are cell numbers in  $x$ - and  $z$ -direction, respectively.  $i = 1, 2, \dots, i_{\max}$ , and  $j = 1, 2, \dots, j_{\max}$ , such that  $\Delta x \cdot i_{\max}$  and  $\Delta z \cdot j_{\max}$  is the size of our grid.

A difference equation relating the state at the time  $t + 1$  with the state at time  $t$  becomes

$$\begin{aligned}
 C_{i,j}^{t+1} - C_{i,j}^t &= - \frac{U_j \Delta t}{\Delta x} (C_{i,j}^t - C_{i-1,j}^t) \\
 &+ (C_{i,j+1}^t - C_{i,j}^t) \left( \frac{K_j + K_{j+1}}{2 \Delta z} \right) \frac{\Delta t}{\Delta z} \\
 &- (C_{i,j}^t - C_{i,j-1}^t) \left( \frac{K_j + K_{j-1}}{2 \Delta z} \right) \frac{\Delta t}{\Delta z}
 \end{aligned} \tag{3}$$

where  $U_j$  and  $K_j$  are respectively velocity and eddy diffusivity at the center of the  $j$ 'th cell.  $\Delta t$  is the constant time step. Equation (3) is valid only with constant steps  $\Delta x$  and  $\Delta z$  throughout the grid and with the conditions  $1 < i < i_{\max}$ ,  $1 < j < j_{\max}$ ,  $t > 0$ .

Boundary conditions give the following relations

$$C_{i,j_{\max}}^{t+1} = C_{i,j_{\max}}^t - 1 \quad \text{and} \quad C_{i_{\max},j}^{t+1} = C_{i_{\max},j}^t - 1, j \tag{4}$$

this allows a simple outflow of material from the grid.

The condition

$$C_{1,j}^{t+1} = C_{1,j}^t = 0, j \neq 1 \quad (5)$$

reflects that there is no transport into the grid from the left side.

The transport equation for the lower left cell is

$$C_{1,1}^{t+1} = C_{1,1}^t \left(1 - \frac{U_1 \Delta t}{\Delta x}\right) + \frac{Q \cdot \Delta t}{\Delta x \Delta z T} \quad (6)$$

for  $0 \leq t \leq T$ , otherwise  $C_{1,1} = 0$

$Q$  is total release.

For  $j = 1, i = 2, \dots, i_{\max} - 1$  we get

$$\begin{aligned} C_{i,1}^{t+1} - C_{i,1}^t &= - \frac{U_1 \Delta t}{\Delta x} (C_{i,1}^t - C_{i-1,1}^t) \\ &+ (C_{i,1}^t - C_{i,2}^t) \left(\frac{K_2 + K_1}{2 \Delta z}\right) \frac{\Delta t}{\Delta t} - R \cdot C_{i,j}^t \end{aligned} \quad (7)$$

where  $R$  is the deposition velocity.

Computational stability is maintained in this scheme with the conditions

$$\frac{U_n \Delta t}{\Delta x} < 1, \quad \frac{K_{j+1} + K_j}{2 \Delta z} \cdot \frac{\Delta t}{\Delta z} < 0.5$$

### 3.1 Pseudodiffusion

This simple method introduces pseudodiffusion, since every time step moves material from one cell to the next. We thus get a faster transport than the transport according to the advection term, regardless of the strength of the wind.

According to Mahoney and Egan (2), this effect can be reduced considerably if a displacement of the center of mass of the material in each cell is introduced.

Let  $\xi_i$  denote the relative displacement of the center of mass within the  $i$ 'th cell, measured from the middle of the cell in the  $x$ -direction.  $\xi_i$  then has a range from  $-0.5$  to  $0.5$  at the left and right boundaries. The nature of the numerical advection process then depends upon the value of the sum

$$\frac{U_j}{\Delta x} \Delta t + \xi_i$$

We now let  $\delta_i$  denote  $\frac{U_j}{\Delta x} \Delta t$

If  $\delta_j + \xi_i < 0$ , no material is transferred out of the  $i$ 'th cell in the  $x$ -direction.

When  $0 < \delta_j + \xi_i < 1$ , some material is transferred to the next cell, and some remains.

For the general case with

$$0 < \delta + \xi_i^t < 1 \text{ and } 0 < \delta + \xi_{i-1}^t < 1$$

we have the following adjustments to the computational scheme:

Replace advection part with

$$C_{i-1,j}^t (\delta_j + \xi_{i-1,j}^t) - C_{i,j}^t (\delta_j + \xi_{i,j}^t)$$

and compute a new relative displacement for the i'th cell with

$$\xi_{i,j}^{t+1} = \frac{1}{2} \left\{ C_{i,j}^t \left[ 1 - (\sigma_j + \xi_{i,j}^t) \right] \cdot (\sigma_j + \xi_{i,j}^t) \right. \\ \left. + C_{i-1,j}^t \left[ -1 + (\sigma_j + \xi_{i-1,j}^t) \right] \cdot (\sigma_j + \xi_{i-1,j}^t) \right\} / C_{i,j}^{t+1} \quad (8)$$

At the boundaries  $\xi_{i,j_{\max}}^t = \xi_{i,j_{\max}-1}^t$  and  $\xi_{i_{\max}j}^t = \xi_{i_{\max}-1,j}^t$ .

This effect must especially be considered for an instantaneous or short lasting release. It becomes of no practical importance when calculating dosage distributions from a semi-continuous release.

4

#### EXAMPLE

We select a line source along the OY-axis with a total release of 100 kg in 60 sec, i e a source strength of  $1.67 \text{ kg m}^{-1} \text{ s}^{-1}$ . We further select  $\Delta x = 20 \text{ m}$ ,  $\Delta z = 6 \text{ m}$ ,  $\Delta t = 1 \text{ sec}$ ,  $u = 4(z/z_1)^{0.2}$  and  $K = 0.3 (z/z_1)^{0.6}$ , where  $z_1 = 1 \text{ m}$ . The program permits selection of arbitrary functions. However, we here use power functions in order to compare with analytical solutions.

The function for u fits quite well our own field observations in near neutral stratification. The expression for K is based on values from literature. Outprints are: concentration distributions at fixed times, total depositions, total cross-sectional mass transports and dosage distributions. A dosage value can be approximated by the concentration value in the same space point from a continuous line source, provided this latter release is of the same amount per sec as otherwise released totally, i e equals 100 units of mass per m per sec.



$$C(x_1 z) = \frac{(m-n+2) Q}{u_1 \Gamma(s)} \left[ \frac{u_1}{(m-n+2)^2 K_1 \cdot x} \right]^s \exp \left[ - \frac{u_1 z^{m-n+2}}{(m-n+2)^2 K_1 \cdot x} \right] \quad (9)$$

where  $u = u_1 z^m$ ,  $K = K_1 z^n$ ,  $s = (m+1)/(m-n+2)$  and  $\Gamma$  is the gamma function.

For  $Q = 100$  mass units

$$C(x, z) = 52.64 x^{-0.75} \exp \left[ -5.21 (z^{1.6})/x \right] \text{mass units}/m^3$$

Figure 1-4 show some computations which illustrates effects of deposition.

Figure 1 shows no apparent difference between computed and theoretical results beyond about 0.7 km. The finite source extention explains the lower computed dosages at shorter distances.

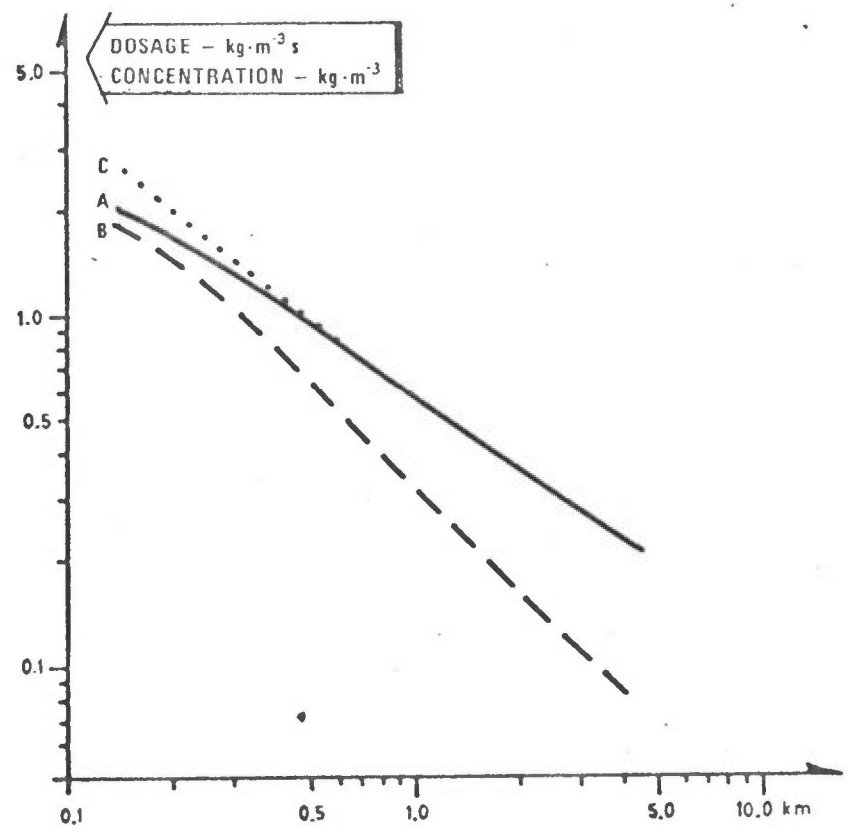


Figure 1 Computed surface dosages and calculated concentrations  
 A - computed dosages - no deposition  
 B - computed dosages - deposition velocity  $0.005 \text{ ms}^{-1}$   
 C - theoretical concentrations from continuous release - no deposition

Figure 2 shows vertical concentration distributions above the 10 m level. At 620 m there is no apparent difference between computed dosages and concentrations. The maximum level is still below 10 m for a deposition velocity of  $0.005 \text{ ms}^{-1}$ . At 4 km there is a difference in computed and theoretical values above 50 m and deposition gives a maximum dosage at 20 m.

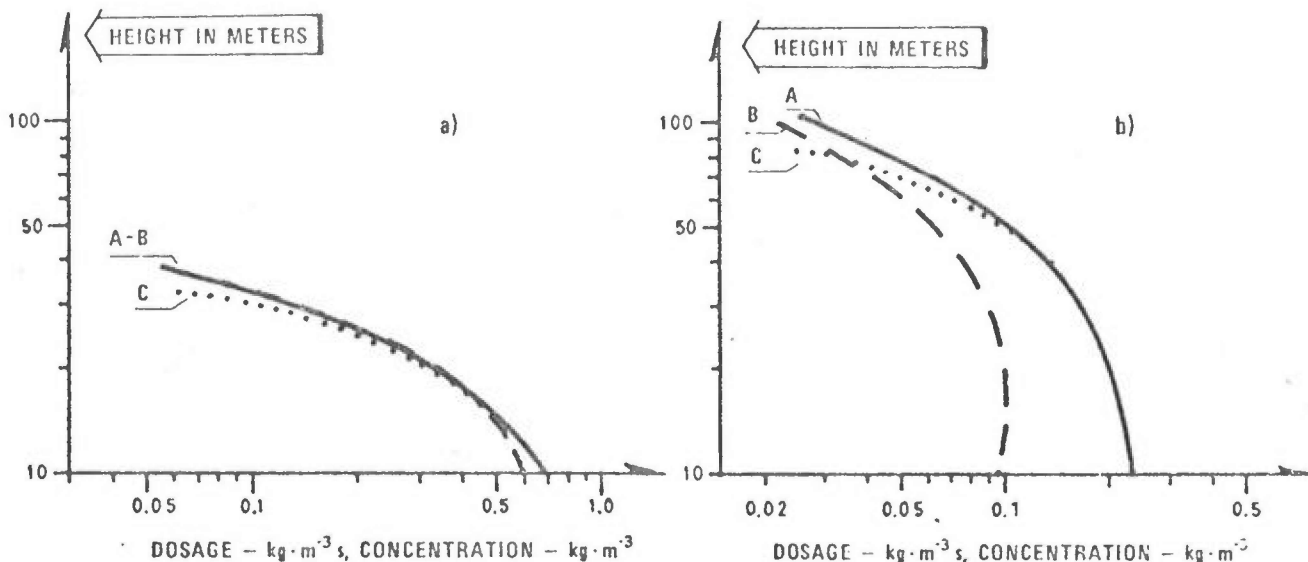


Figure 2 Computed vertical dosage and calculated concentration distributions at 620 m (a) and at 4 km (b)  
 A - computed dosages - no deposition  
 B - computed dosages - deposition velocity  $0.005 \text{ ms}^{-1}$   
 C - theoretical concentrations from continuous release - no deposition

The difference between maximum flux and concentration levels is illustrated in Figure 3, which shows outlines of the cloud.

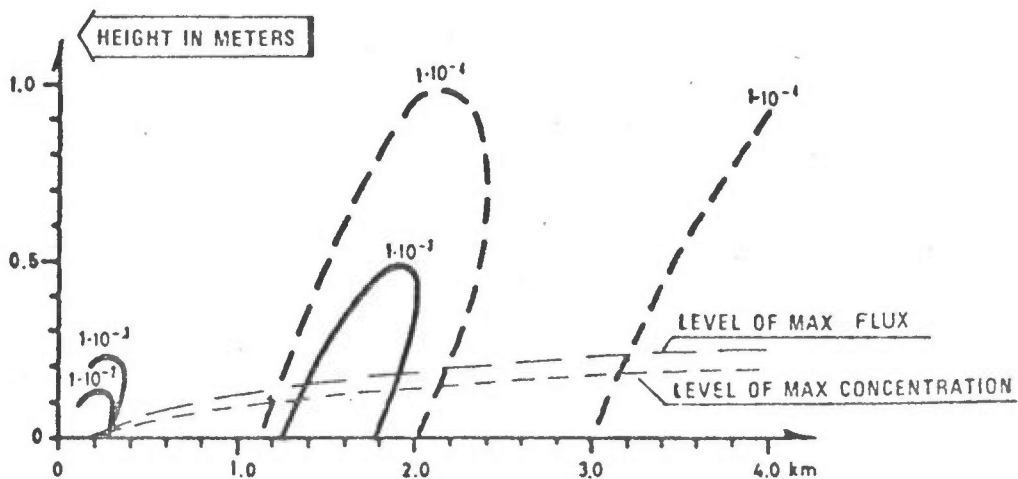


Figure 3 Computed concentration distributions - level of computed maximum concentration and dosage distribution  
 Deposition velocity  $0.005 \text{ ms}^{-1}$

Finally, Figure 4 shows the decrease in total cross-sectional flux with distance, due to deposition. The decrease is high close to the source, but the flux gets nearly constant already beyond a few kilometers.

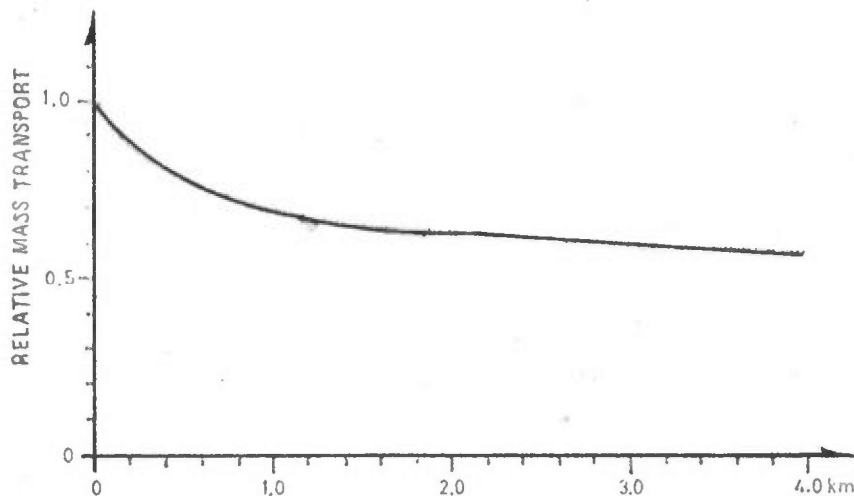


Figure 4 Total mass passing through a cross-section  
Relative values - deposition velocity  $0.005 \text{ ms}^{-1}$

The Mahoney - Egan method to reduce pseudodiffusion was applied to obtain Figure 3. But when we used this method to compute dosages and fluxes, we could not detect any difference in the distributions from the other more direct method.

#### References

- (1) Monin, A S  
A M Yaglom  
- Statistical Fluid Mechanics:  
Mechanics of turbulence - Vol 1  
MIT PRESS Cambridge, Mass and  
London (1971)
- (2) Egan, B A  
J R Mahoney  
- A numerical model of urban air  
pollution transport. Reprints  
of Papers, Conf Air Pollution  
Meteorology, Raleigh, N C, Amer  
Meteor Soc (1971)

APPENDIX

COMPUTING TECHNIQUE

In the computer program based on the preceding scheme, 3 matrixes of data have to be updated: the concentrations (C-matrix), relative displacement (XSI-matrix) and the accumulated flux in each cell (ACC-matrix).

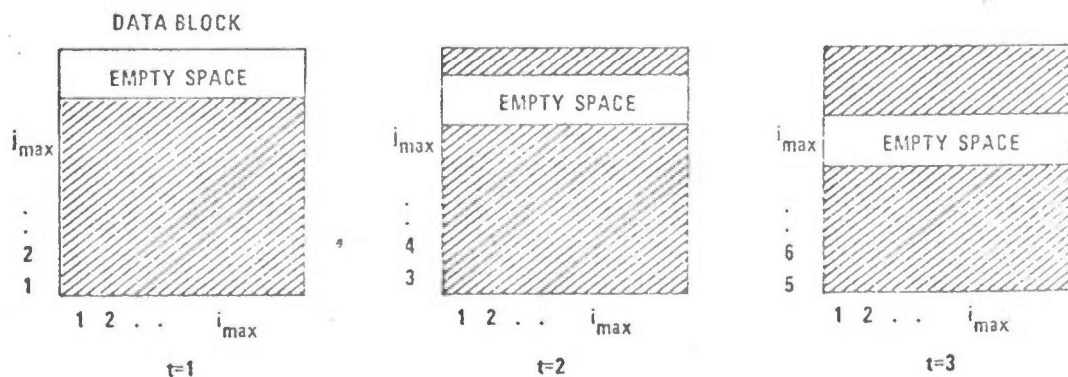
The simplest way to do this is to have two copies of each matrix, one for time t, and another for time t+1.

The value in  $C^{t+1}$  can then be computed from  $C^t$  (and eventually  $XSI^t$ ). In the next computation, we have  $C^{t+1}$  as the old one and (we) can store values for time t+2 into the former  $C^t$ . The same method can be applied for XSI and ACC. This method is, however, very storage-consuming, and thus restrictive regarding the number of grid elements.

In our program we have therefore used another method, which requires some extra computing time, but only half the data space.

Equations (3) and (8), show that the new values computed are based on nearest neighbours in the grid. Thus, if we update the matrixes from bottom to top, we may very well store new values in the same matrix as long as we do not destroy the values needed in computing values for the next cell.

Extra lines are therefore added in the matrixes, and used in a roll-around fashion, as shown below. At least two extra lines are needed.



The outprints from this program are:

- C-matrix - Concentration distribution  $C(x,z,t)$  at fixed times  $t$
- Condensed - Total depositions after a time  $T$  in the range  $x = 0$  to  $x = K \cdot \Delta x$   
Amount =  $\sum_{t=0}^T \sum_{i=1}^K R \cdot C_{i,l}^t$
- Remaining - Total amount of mass passing the cross-section at  $x = K \cdot \Delta x$   
Amount remaining = 1-condensed  $(x,T)$
- Concentrations - An isograph plot of the concentration distribution at fixed times  $t$
- Integral - Total mass passing through a cell =  $D \cdot u$
- Mean con - Mean concentration, i e dosage distribution  $D(x,z)$